External Grant Award No.: 03HQGR0065

HIGH-RESOLUTION MONITORING AT PARKFIELD

Program Elements: **I, II**

Principal investigator, author:
Robert M. Nadeau
Berkeley Seismological Laboratory
University of California, Berkeley
211 McCone Hall, MC: 4760,
Berkeley, CA 94720-4760
Tel: (510) 643-3980
Fax: (510) 643-5811
e-mail: nadeau@seismo.berkeley.edu

Recipient:
University of California - Berkeley

Research supported by the U.S. Geological Survey (USGS), Department of the Interior, under USGS award number 03HQGR0065. The views and conclusions contained in this document are those of the authors and should not be interpreted as necessarily representing the official policies, either expressed or implied, of the U.S. Government.

External Grant Award No.: 03HQGR0065

HIGH-RESOLUTION MONITORING AT PARKFIELD

Robert M. Nadeau, University of California, Berkeley Seismological Laboratory, Berkeley CA 94720-4760
Telephone: (510) 643-3980, FAX: (510) 643-5811, nadeau@seismo.berkeley.edu

NEHRP Elements: I, II. Keywords: Source characteristics, Fault dynamics, Fault stress interactions, Earthquake forecasting

Non-Technical Project Summary

This project addresses the seismic potential hazard presented by large earthquakes on the San Andreas Fault system using numerous small earthquakes. It provides waveform and catalog data of very low magnitude seismicity in the region surrounding the magnitude 6 locked zone at Parkfield, CA. It provides general information on earthquake source properties, on the detailed structure of the San Andreas fault, on the spatio-temporal distribution of deep fault slip, and on fault roughness and strength. It also directly contributes to NSF's EarthScope initiative "SAFOD" and to the development of time-dependent earthquake forecast models by providing earthquake recurrence data.

External Grant Award No.: 03HQGR0065

HIGH-RESOLUTION MONITORING AT PARKFIELD

Principal investigator, author:
Robert M. Nadeau
Berkeley Seismological Laboratory
University of California, Berkeley
211 McCone Hall, MC: 4760,
Berkeley, CA 94720-4760
Tel: (510) 643-3980
Fax: (510) 643-5811
e-mail: nadeau@seismo.berkeley.edu

TECHNICAL ABSTRACT

A high quality borehole seismometer network in place at Parkfield has fostered the evolution of a new and exciting view of San Andreas fault-zone processes as they respond to plate-boundary loading. The observational data and scientific inferences from this research project have been catalytic in spawning wide-ranging analyses and arguments over the fine-scale processes underway on seismogenic fault zones. Our continuing studies at Parkfield demonstrate conclusively the existence of an extremely regular process of repeating earthquakes whose recurrence interval variations through space and time reflect deep fault slip rate variations. We do not yet fully understand the relationship of these variations to the M6 nucleation process but the unique findings so far have significant implications for source dynamics, for earthquake forecasting, and for scaling relations among source parameters such as fault slip, rupture dimension, stress drop and seismic moment. Compelling evidence also exists for changes with time in seismicity and in wave propagation (from repeating microearthquake and Vibroseis sources) that appear to be coupled, and the region of the fault zone involved is the presumed M6 nucleation volume SE from Middle Mountain. Synchronous changes well above noise levels have been seen among several parameters including seismicity rate, average focal depth, S-wave coda velocities, characteristic micro-quake recurrence intervals, fault creep and water levels in monitoring wells, and the scattering field. Recurrence-time variations in repeating sequences of small earthquakes have now been found elsewhere in the San Andreas system, including faults in the Bay Area, Japan and Taiwan, providing a new method for monitoring the changing strain field throughout the seismogenic zone.

Data and research results from this network provide fundamental input for models of time-dependent earthquake forecasts, on spatial-temporal clustering of earthquakes, on triggering of events, and on the systematic variations of deep slip rate in active fault zones. Additionally, the real-time monitoring of fault-zone process provides one of the rare hopes for understanding and tracking the nucleation of potential damaging earthquakes, an outcome, if eventually realized, that would aid significantly in reducing losses from earthquakes.

The major investment in time and money put into the high resolution seismic monitoring effort since late 1986 has produced a unique baseline of fault-zone behavior with distinct features observed rather than theorized, a body of observations that must be incorporated in new models for fault-zone deformation. Late in 1998 the 1980-vintage acquisition hardware finally

recorded its last Parkfield microearthquake and failed irreparably. Assistance from the IRIS/PASSCAL instrument pool brought the system online in a stopgap mode. In 1999 NEHRP funds were made available to replace the system with new 24-bit data flowing seamlessly into the NCEDC data center, where the 1987-98 Parkfield data base resides. NSF funds were also provided to expand the borehole network with 3 new stations in the vicinity of the planned EarthScope/SAFOD experiment. The upgrade and expansion efforts were completed this year and sustained operation of the 13 borehole station HRSN is helping to characterize seismic behavior in the target region of the SAFOD fault-zone drilling project. We have continued to executed a basic program of operation and maintenance of the network and have continued our research program using the data in the study of the spatio-temporal details of microearthquake dynamics, wave propagation and slip-rate variations. The new hardware, additional three SAFOD borehole sensors, and refinement of the triggering algorithm have reduced the detection threshold of the network to M<-1.0 in the central region around SAFOD. Due to the networks extreme sensitivity for detecting very low amplitude seismic events, aftershocks from the M6.5 San Simeon earthquake of December 22, 2003 have complicated the task of identifying Parkfield local events from regional non-local seismicity. We are now exploring alternatives to our data processing scheme to allow us to overcome the aftershocks problem.

NON-TECHNICAL ABSTRACT

This project addresses the seismic potential hazard presented by large earthquakes on the San Andreas Fault system using numerous small earthquakes. It provides waveform and catalog data of very low magnitude seismicity in the region surrounding the magnitude 6 locked zone at Parkfield, CA. It provides general information on earthquake source properties, on the detailed structure of the San Andreas fault, on the spatio-temporal distribution of deep fault slip, and on fault roughness and strength. It also directly contributes to NSF's EarthScope initiative "SAFOD" and to the development of time-dependent earthquake forecast models by providing earthquake recurrence data.

A high quality borehole seismometer network in place at Parkfield has fostered the evolution of a new and exciting view of the San Andreas fault-zone processes as it responds to its plate-boundary loading. The observational data and scientific inferences from this research project have been catalytic in spawning wide-ranging analyses and arguments over the fine-scale processes underway on seismogenic fault zones. Our ongoing studies at Parkfield demonstrate conclusively the existence of an extremely regular and localized process of ongoing earthquake-accommodated slip in the fault zone. Plausible assumptions lead to estimates for the spatial distribution of variations in slip-rate on the deep fault surface from 2000+ characteristic microearthquakes. The unique findings so far have significant implications for earthquake source dynamics, for earthquake forecasting, and for scaling relations among earthquake source parameters. Compelling evidence also exists for changes with time both in seismicity and in wave propagation that appear to be coupled, and the region of the fault zone involved is the presumed nucleation volume of the repeating M6 sequence of events at Parkfield. Sequences of near-identically repeating small earthquakes in the area are also providing a new method for monitoring the changing strain field throughout the seismogenic zone.

Data and research results from this network provide fundamental input to models of earthquake forecasting, on spatial-temporal clustering of earthquakes, on triggering of events, and on the systematic variations of slip rate on an active fault. This information is critical to earthquake risk estimation. The real-time monitoring of these fault-zone processes provides one of the rare hopes for understanding and tracking the nucleation of potential damaging earthquakes, an outcome, if eventually realized, that would be do much in reducing losses from earthquakes.

A major investment of time and money has produced a unique baseline of fault-zone behavior with distinct features observed rather than theorized, a body of observations that must be incorporated in new models for fault-zone deformation. Late in 1998 the 1980-vintage hardware finally recorded its last Parkfield microearthquake and failed irreparably. Assistance from the IRIS/PASSCAL instrument pool brought the system online in a stopgap mode. In 1999 NEHRP funds were made available to replace the system with new 24-bit data flowing seamlessly into the NCEDC data center, where the 1987-98 Parkfield data base resides. NSF funds were also provided to expand the borehole network with 3 new stations in the vicinity of the planned EarthScope/SAFOD experiment. The upgrade and expansion efforts were completed this year and sustained operation of the 13 borehole station HRSN is helping to characterize seismic behavior in the target region of the SAFOD fault-zone drilling project. We have continued to executed a basic program of operation and maintenance of the network and have continued our research program using the data in the study of the spatio-temporal details of microearthquake dynamics, wave propagation and slip-rate variations. The upgrade, expansion and other refinements that we have implemented have reduced the detection threshold of the network to

M<-1.0 in the central region around SAFOD. Due to the networks extreme sensitivity for detecting very low amplitude seismic events, aftershocks from the M6.5 San Simeon earthquake of December 22, 2003 have complicated the task of identifying Parkfield local events from regional non-local seismicity. We are now exploring alternatives to our data processing scheme to allow us to overcome the aftershocks problem

FINAL TECHNICAL REPORT:

HIGH-RESOLUTION MONITORING AT PARKFIELD

Introduction

As part of the U.S. Geological Survey initiative known as the Parkfield Prediction Experiment (PPE) (Bakun and Lindh, 1985), the operation of the High Resolution Seismic Network (HRSN) at Parkfield, California, and the collection and analysis of its recordings began in 1987. Figure 1 shows the location of the network, its relationship to the San Andreas Fault, sites of significance to previous and ongoing research using the HRSN, relocated earthquake locations, and the epicenter of the 1966 M6 earthquake that motivated the PPE. The HRSN records exceptionally high-quality data, owing to its 13 closely spaced three-component borehole sensors, its very wide band-width high frequency recordings (0-100 Hz), and its sensitivity (recording events below magnitude -1.0) due to the extremely low attenuation and background noise levels at the 200-300 m sensor depths (Karageorgi et al., 1992). Several aspects of the Parkfield region make it ideal for the study of small earthquakes and their relation to tectonic processes. These include the fact that the network spans the expected nucleation region of a repeating magnitude 6 event and the transition from locked to creeping behavior on the San Andreas fault, the availability of three-dimensional P and S velocity models, a very complete seismicity catalogue, a well-defined and simple fault segment, a homogeneous mode of seismic energy release as indicated by the earthquake source mechanisms (over 90% right-lateral strike-slip), and the planned drilling zone and penetration and instrumentation site of the SAF deep observatory at depth (SAFOD) installation.

Scientific Significance. The problem addressed in this research has always been to improve our understanding of fault zone dynamics at very high resolution (meters) and to develop precise characterization methods that will allow monitoring of the subtle changes in process and properties underway within a seismogenic fault zone. Data and research results from this network are providing fundamental input to models of earthquake recurrence, on spatial-temporal clustering of earthquakes, on triggering of events at distance, on earthquake scaling and physics, on fault strength and heterogeneity, and on the systematic variations of slip rate and strain accumulation on an active fault, information critical to earthquake risk estimation and loss mitigation. Throughout its 17 years history, the Parkfield High-Resolution Seismic Net (HRSN) has acquired unique data that are forcing a new look at several conventional concepts and models for earthquake occurrence and mechanisms, and has provided a baseline and characterization of seismic activity complete down to very low magnitudes that has proven critical to many previous and ongoing studies (e.g. the SAFOD component of EarthScope).

This research began with NEHRP in 1986 as a proposed direct test with proven and modern technology of two hypotheses critical to our understanding of the physics of the earthquake process, implications for earthquake hazard reduction, and the possibilities for short-term earthquake prediction - major goals of the NEHRP:

1) That the earthquake nucleation process produces stress-driven perturbations in physical properties of the rocks in the incipient focal region that are measurable, and

2) That the nucleation process involves progressive and systematic failure that should be observable in the ultralow-magnitude microseismicity with high-resolution locations and source mechanisms.

Little did we know then about the power of borehole networks, where remarkably low noise levels opened a window on the realm of microearthquake observations at M<0 and frequencies to 100 Hz. This unprecedented resolution has driven our research (and that of many colleagues) for the past decade, with many exciting discoveries. In a series of journal articles and Ph. D. theses, we have presented the cumulative, often unexpected, results of this effort. They trace the evolution of a new and exciting picture of the San Andreas Fault zone responding to its plate-boundary loading, and they are forcing new thinking on the physics and structure of earthquake faults in general and on dynamic processes and conditions within the fault zone at the sites of recurring small earthquakes.

Analyses of the Parkfield monitoring data have revealed significant and unambiguous departures from stationarity both in the seismicity characteristics and in wave propagation details. Within the presumed M6 nucleation zone we have found a high Vp/Vs anomaly at depth (Michelini and McEvilly, 1991), where the three M4.7-5.0 sequences occurred in 1992-94 and, more recently, where an anomalously high Q region in the fault zone appears through tomographic analysis to be the source volume where the fault-zone guided waves (FZGW) are generated (Korneev et al., 2003). Synchronous changes well above noise levels have been seen among several independent parameters, including seismicity rates, average focal depth, S-wave coda velocities, characteristic sequence recurrence intervals, fault creep and water levels in monitoring wells (Karageorgi et al., 1997). We have been able to localize the S-coda travel-time changes to the shallow part of the fault zone and demonstrate with numerical modeling the likely role of fluids in the phenomenon (Korneev et al., 2000). This zone is also the upper part of the FZGW generation volume. We can connect the changes in seismicity to slip-rate variations evident in other (strain, water level) monitored phenomena.

New and unconventional scaling laws have been developed from the Parkfield earthquakes that can be projected to fit earthquakes up to M6 (Nadeau and Johnson, 1998) and to fossil earthquakes (pseudotachylite structures) of magnitudes as small as -2Mw (Wenk et al., 2000) and they predict unprecedented high stress drops and melting on the fault surface for the smallest events. The exhumed fault-zone rocks (pseudotachylite-melt) provide independent evidence for such conditions. A new asperity model for earthquakes has been developed that explains these new scaling laws (Johnson and Nadeau, 2002). Recurrence interval variations in the characteristic event sequences (> 40% of the microearthquake population) have been used to map fault slip rate at depth on the fault surface (Nadeau and McEvilly, 1999), and decomposition of the total seismicity into repeating and non-repeating seismicity has revealed a discrepancy in their b-value statistics suggesting a greater fraction of large earthquakes repeat characteristically relative to smaller quakes (Johnson and Nadeau, 2002). Along the way in this exciting discovery process we have challenged the conventional 'constant stress drop' source model, affirmed characteristic earthquake occurrence and demonstrated the ability to detect and track temporal changes in fault-zone properties. The significance of these findings lies in their apparent coupling and inter-relationships with surface deformation, from which models for fault-zone dynamics can be fabricated and tested.

The more general significance of the project is its production of a truly unique continuous baseline, at very high resolution, of both the microearthquake pathology and the subtle changes

in fault-zone environment at depth. These data are openly available to researchers on the NCEDC archive, and provide the seismological community an earthquake laboratory available nowhere else. This unique body of observations and analyses has also provided much of the impetus for Parkfield as the preferred site for deep drilling into an active seismogenic fault zone (SAFOD). The network has recently completed a total hardware upgrade to modern real-time telemetry and data flow into the BDSN stream, and, with NSF support, the addition of three new borehole stations to better focus on the SAFOD drilling target. With the upgrade, expansion and other enhancements, the detection threshold of the HRSN in the SAFOD zone is now less than -1.0Mw, providing a complete baseline of very low magnitude microseismicity to aid in the operational and research objectives of SAFOD.

Reducing losses from Earthquakes in the U.S. A better understanding of earthquake physics, processes and recurrence models are critical to reducing losses from earthquakes in the U.S., and our research is arguably fundamental to those goals. Results obtained from this data collection and research effort provide unique information on the strain accumulation on faults at depth, estimation of the strength and strength heterogeneity of earthquake generating faults (i.e. fault roughness), and on scaling properties of earthquake recurrence times and rupture parameters, all of which are critical input for accurate earthquake forecasts, fault rupture models, and ground motion and earthquake hazard estimation. Uniquely, through the study of characteristically repeating small earthquakes this work also promises to provide direct tests of earthquake forecast models by making predictions based on these models and assessing their success rates on time scales of months to a few years as opposed to decades to centuries as required for similar tests using large magnitude events.

Recent Activities

Over the past year, activities associated with the operation of the HRSN primarily involved five components: 1) routine operations and maintenance of the network, 2) enhancement of the network's performance for detection and recording of very low amplitude seismic signals, 3) repair of the severed 48 pair cable at the VARB site, 4) collaborative integration and analysis of HRSN and SAFOD's temporary deployments for refining the structure and target location estimates in the SAFOD drill path, 5) data processing and analysis of the pre-San Simeon, and post-San Simeon data.

Operations and Maintenance: In addition to the routine maintenance tasks required to keep the HRSN in operation, various refinements and adjustments to the networks infrastructure and operational parameters have been needed this year to enhance the HRSN's performance and to correct for pathologies that continue to manifest themselves in the recently upgraded and expanded system. A feature of the new system that has been particularly useful both for routine maintenance and for pathology identification has been the internet connectivity of the central site processing computer and the station data loggers with the computer network at BSL. Through this connection, select data channels and on-site warning messages from the central site processor are sent directly to BSL for evaluation by project personnel. If, upon these evaluations, more detailed information on the HRSN's performance is required, additional information can also be remotely accessed from the central site processing computer at Parkfield. Analysis of this remotely acquired information has been extremely useful for trouble shooting by allowing field personnel to schedule and plan the details of maintenance visits to Parkfield. The

connectivity also allows certain data acquisition parameters to be modified remotely when needed, and commands can be sent to the central site computer and data loggers to modify or restart processes when necessary.

The network connectivity also allows remote monitoring of the background noise levels being recorded by the HRSN stations. For example shown in Figure 2 are power spectral density plots of background noise for vertical components of the 7 HRSN stations that are most critical for monitoring seismicity in the region containing SAFOD. The PSD analysis gives a rapid assessment of the HRSN seismometer responses across their wide band-width. By routinely generating these plots with data telemetered from Parkfield, changes in the seismometer responses, often indicating problems with the acquisition system, can be easily identified, and corrective measures can then be planned and executed on a relatively short time frame.

Smaller scale maintenance issues addressed this year include cleaning and replacement of corroded electrical connections, grounding adjustments, cleaning of solar panels, re-seating, resodering and replacement of faulty pre-amp circuit cards, and the testing and replacement of failing batteries. Larger efforts included the implementation of periodic emergency generator tests, replacement of the central site air conditioning unit, a major insulation, painting and power enhancement effort at our Gastro Peak repeater site to address problems with outages and low power during cold weather, and a switch to an alternative sensor on the VARB station deep string due to the failure of one of the 1877' deep sensor components.

Enhancing HRSN Performance: Over the past year significant efforts were made to identify and reduce noise problems arising from the new and expanded data acquisition system. Detection, monitoring, and high-resolution recording of earthquakes down to the smallest possible magnitudes with the highest possible signal-to-noise (especially in the region of the proposed SAFOD drilling) is a major objective of the HRSN data collection effort. Consequently, elimination of all sources of unnaturally occurring system noise is a primary goal. The minimization of data loss due to station outages and data-dropouts is also critical to this objective.

The sophisticated HRSN data acquisition involves integration of a number of distinct components at each station (i.e., sensor, pre-amp, solar panels, solar regulator, batteries, Freewave radio, antenna, lightening arresters, and associated cabling, connectors and grounds) and radio telemetry apparatus between the seismic stations, telemetry relay stations, and the central processing site on the CDF site in Parkfield. This complex integration of station and communication components combined with a variety of associated concerns (e.g., ground loops, cable resistances, radio feedback into recording equipment at stations, radio interference between stations, marginal line of site paths, cloud cover and solar power, the integration of older (pre-upgrade) hardware components with new components, old component deterioration and failures, and malfunctioning and unexpected performance characteristics of newer components) all make identification of specific causes of network generated (i.e. artificial) noise difficult to identify. Exhaustive and iterative testing of HRSN performance has identified two primary causes for observed artificial noise remaining in the system (i.e. solar regulator spiking and pre-amp self-noise generation). Over the past year we have designed and have implemented fixes for these problems.

Solar Regulators. Regularly occurring spikes occurring during the daylight hours were observed in the continuous data streams and found to be due to the solar regulators. We have

tested a variety of solar regulator designs and have identified the Prostar 30 as having the optimal cost-benefit. We have purchased and installed several of these devices at several of the HRSN sites with the ultimate goal of installing the Prostar's at all the HRSN stations as time and funding permit.

Pre-amplifier Noise. We found that a significant source of artificial noise was coming from the station pre-amplifiers. In the upgraded system, pre-amps from the older network were used. During integration of the older pre-amps with the increased dynamic range capabilities of the 24-bit Quanterra system, gain settings of the pre-amps were reduced from x10,000 to x80 in order to match signal sensitivity of the new system with the older one. While these lower pre-amp gain levels are still within the operational design of the pre-amps, they are no longer in their optimal range and a significant contribution of preamp's self-generated noise is present in the recorded seismograms. Initially, this was not expected to be a significant problem. However, we have subsequently found that even the small increase in pre-amp noise that results from the pre-amp gain reduction significantly impacts the sensitivity of the network for detecting and recording the smallest locatable events.

Figure 3 shows the pre-amp noise reduction effect observed on background noise signals at three vertical components of the HRSN when gains are raised from x80 to x1,000. Considerable signal hash is seen at gain levels of x80 (top waveform in each station pair), and significantly reduced when gains are increased to x1,000 (lower waveforms). Since we are also interested in recording large earthquakes on-scale, simply increasing gain levels on all stations is not the preferred solution, since doing so causes the recording system to saturate at much lower magnitudes. Instead we are attempting to redesign the pre amps using modern components to reduce the noise levels at the lower gain levels. However our attempts at redesign have not yet yielded satisfactory results.

Since a primary objective of the HRSN is to monitor the evolving patterns of the numerous small earthquakes that occur at very low magnitudes, and since this objective also complements the scientific objectives of the recently funded SAFOD experiment, it is important to address the pre-amp noise problem in a timely manner. We have opted, therefore, to raise the gain levels for the near-term on all the station pre-amps from x80 to x1,000. By early October of 2003, these gain changes were implemented at all 13 HRSN stations. Plans are to continue investigating pre-amp redesigns until a suitable alternative is found at which time we will install the new pre-amps and lower the pre-amp gain back to x80--allowing both the increased detection of small events and the on-scale recording of events up to about magnitude 4 to 4.5.

<u>*Repairs at VARB:*</u> The borehole HRSN plays an important role in the Parkfield Prediction Experiment and in the seismic characterization of the region surrounding SAFOD. In July or 2003 our group began having trouble with the recording of data at one of the HRSN stations (VARB) located at the Varian well site on Jack Varian's property. After contacting the USGS field technician at Parkfield we were informed that the sensor cable to the seismic string down the Varian well had been severed as part of a cleanup effort at the Varian well site. This activity not only cut the connection to the 1877' deep sensor that we had been recording, but also severed connection to the full seismic string of functional seismometers and accelerometers that existed down the deep VARB borehole.

During prior planning of the cleanup effort, we made it clear that it was important to retain connectivity to the seismic sensors at VARB, and the importance of this fact was acknowledged

by the USGS personnel managing the effort. Subsequent plans for the cleanup specified coordination of the effort with field personnel from UC Berkeley. Nonetheless, Berkeley was not notified of the date the cleanup was to take place, nor of the specifics of the cleanup plan which apparently included severing the deep strings cable at the well head (which of course we would have loudly objected to). Because VARB has the deepest HRSN borehole sensor and is centrally located within the network, it is a critical site for the HRSN. In addition at that time, we were in the process of preparing VARB and all the HRSN stations to make high-gain recordings of the controlled source shots from the SAFOD related 50 km line experiment to aid in characterizing the velocity and Fault Zone Guided Wave propagation structure in the region around SAFOD. Needless to say, the unpleasant circumstances arising from the cleanup effort severely hampered these efforts. The situation was further complicated by the details of how the Varian well cable disconnect was made.

It was important for a number of scientific reasons to reconnect our VARB acquisition system to a sensor of known depth. However, there are some 48 pairs of wires in the seismic string cable that was severed, and unfortunately, the mapping of these wires to their corresponding sensors was not documented when the cable was severed. In addition because the cable was severed at the well head, some 100' of trenching and cable was needed to reconnect the sensor and recording installation. The estimated cost for the additional man-hours, parts, travel and lodging needed to do the necessary repairs at VARB was several thousand dollars and this put an unmanageable burden on our already meager O & M budget. It was necessary, therefore, to request emergency funding from NEHRP to perform the repairs. Our funding request was granted and with assistance from the USGS field technician at Parkfield we put VARB back on-line and made the high-gain HRSN adjustments in time for the 50 km line experiment shots.

SAFOD Collaboration: The San Andreas Fault Observatory at Depth (SAFOD) is a comprehensive project to drill into the hypocentral zone of repeating M ~ 2 earthquakes on the San Andreas Fault at a depth of about 3 km. The goals of SAFOD are to establish a multi-stage geophysical observatory in close proximity to these repeating earthquakes, to carry out a comprehensive suite of downhole measurements in order to study the physical and chemical conditions under which earthquakes occur and to exhume rock and fluid samples for extensive laboratory studies (Hickman et al., 2004). The HRSN's unique contributions to SAFOD are: 1) its collection of high-resolution earthquake monitoring data from the numerous very low magnitude earthquakes in the SAFOD zone, 2) its long-term archive of micro- and repeating-earthquake data (extending back to early 1987) occurring over the broader region surrounding SAFOD, and 3) the large body of accumulated scientific knowledge based, in part or entirely, on HRSN data.

An intensive and ongoing effort by the SAFOD target event location working group is underway with its goals being: 1) the characterization of the detailed velocity and seismicity structure in the crustal volume containing the SAFOD main hole and 2) to determine the most accurate estimates of the absolute locations of SAFOD's target events. As part of this effort a series of coincident active and passive source seismic experiments was performed during Oct. - Nov. of 2003. The HRSN data played a key role in this effort by providing complementary seismic waveform data from the active sources and by providing a backbone of earthquake detection, waveform, and location data from the numerous microearthquakes that occurred within the SAFOD local zone during the Oct. 15 through Nov. 11 experimental period (i.e. 256 events within 5 km of the SAFOD target(s)). In a special section of Geophysical Research

Letters from May of 2004, several papers making significant use of the HRSN data for characterizing the SAFOD area have already been published and illustrate the role that the HRSN data have played in the SAFOD effort over the past year. (Oye et al., 2004; Roecker et al., 2004; Thurber et al., 2004; Nadeau et al., 2004).

Seismic Data Processing: Monitoring the evolution of microseismicity, particularly in the SAFOD drilling and target zone, is a primary objective of the HRSN project. In addition, the continued analysis of the HRSN data for determining detailed seismic structure, for the study of similar and characteristic microearthquake systematics, for estimation of deep fault slip rate evolution, and for various studies of fault zone and earthquake physics is also of great interest to seismologists. Before advanced studies of the Parkfield microseismicity can take place, however, initial processing, analysis and routine cataloging of the earthquake data must be done. An integral part of this process is quality control of the processed data, including a final check of the routine catalog results. The numerous aftershocks from the M6.5 San Simeon earthquake have seriously complicated the tasks of initial processing, analysis and location of the routine event catalog. And, a significant revision of the "traditional' processing scheme we have used since 1987 will be required to deal with the post-San Simeon data. We have requested funding for this effort in a proposal to EarthScope, and if granted our intent is to more fully develop, test and implement the new procedures for processing of these data.

Most of our efforts during the 2000 to 2002 period were spent on implementing the emergency upgrade and SAFOD expansion of the HRSN, and routine processing of the data collected during that period was deferred until after upgrade and installation efforts were completed. In 2003 we began in earnest the task of routine processing of the ongoing data that was being collected. Our initial focus was on refining and developing our processing procedures to make the task more efficient and to ensure quality control of the processed catalogs. We also began working back in time to fill in the gap that developed during the deferment period. Because routine processing of the post-San Simeon data is effectively impossible at this time because of the overwhelming number of aftershocks, we have suspended our efforts at processing the ongoing data and focused our efforts at filling in the complete gap of unprocessed data (i.e., back to March of 2001). Outlined below in the "Pre-San Simeon Processing" subsection are the procedures and issues related to this effort. In the subsequent subsection we illustrate and discuss briefly the issues that need to be addressed in order to process the post-San Simeon event data.

Pre-San Simeon Processing.

Initial Processing. Continuous data streams on all 38 HRSN components are recorded at 20 and 250 sps on disk on the local HRSN computer at the CDF facility. The 20 sps data are transmitted continuously to the Berkeley Seismological Laboratory (BSL) over a frame-relay link and then archived at the NCEDC. In addition, the vertical component channels for the 7 stations critical to resolving seismicity in the SAFOD area are also being transmitted continuously to the BSL at 250 sps over the frame relay-circuit for purposes of quality control and fine tuning the triggering algorithm for the detection of the smallest possible events around SAFOD. These telemetered 250 sps data are archived on disk for only about 1 week at the BSL and are then deleted. When the local HRSN computer disk space is full, the continuous 250 sps data on the HRSN local computer are migrated onto DLT tape, and the tapes sent to Berkeley for long-term storage and for data upload to the NCEDC archive in some cases.

Shortly after being recorded to disk on the central site HRSN computer, event triggers for the individual station data are determined and a multi-station trigger association routine then processes the station triggers and identifies potential earthquakes. For each potential earthquake that is detected, a unique event identification number (compatible with the NCEDC classification scheme) is assigned. Prior to San Simeon earthquake of December 22, 2003, 30 second waveform segments were then collected for all stations and components and saved to local disk as an event gather, and event gathers were then periodically telemetered to BSL and included directly into the NCEDC earthquake database (dbms) for analysis and processing.

An ongoing effort has been the development of a new earthquake detection scheme, with the goal of routinely detecting SAFOD area events to magnitudes below -1.0. A first cut version of the new scheme has been implemented and is currently detecting real earthquakes at an increased rate--nearly 3 times the number of earthquakes detected before the upgrade. In order to facilitate the processing and archiving of the increased number of potential earthquakes (~ 350 per month), the BSL has recently developed a Graphical User Interface (GUI). The GUI is integrated with the NCEDC dbms and allows review of the waveforms from every potential event. Initial analysis of the data using the GUI involves review of the waveforms and classification of the event as an earthquake or non-earthquake. The GUI also allows the analyst to log potential network problems that become apparent from the seismograms. The HRSN analyst then classifies the earthquakes as either a local, distant-local, regional, or teleseismic event and then systematically hand picks the P- and S-phases for the local and distant local events (for the period Sept. 2002 - Aug. 2003 the number of picked events was ~ 2000).

Picking of the numerous microearthquake events is no mean task. On average about 7 P-phases and 4 S-phases are picked for each event, putting the total number of annual phase picks for the HRSN data on the order of to 22,000. We have experimented with algorithms that make initial auto-picks of the phase arrivals, but have so far found picking by hand to be significantly more accurate and has the added advantage of allowing the analyst to assess the state of health of each station-component. In all our tests, autopicks have also invariably resulted in some missed events and catalog locations that are significantly more scattered and with higher residuals than locations done with purely hand-picked data.

A peculiarity of processing very small earthquake data, is that multiple events commonly occur within a few seconds of one another. The close timing of these events does not allow the local triggering algorithm to recover from one event before another occurs. As a result, the central site processor often does not trigger uniquely for each event. In such cases only one, 30 sec waveform gather and one earthquake identifier will be created for all the events. These multiple earthquake records (MER) account for only 3 to 5 % of the total seismicity recorded by the HRSN. However, there are times when this rate rises to over 10 %. In order to assign each event in an MER a unique event identifier for the NCEDC dbms and to make picking and automated processing of these events more manageable an additional feature of the GUI was developed that allows the analyst to "clone" MER into separate gathers for each event.

Quality Control. Once false triggers have been removed and picks for the local and distant local events have been completed, quality control on the picks is made to ensure that all picks have phase and weights assigned, that extraneous characters have been removed from the pick files, that double station-phase picks have not inadvertently been made, and that no repicks of the same event had been accidentally made during any cloning that was performed. Initial locations are then performed and phase residuals analyzed in order to determine whether severe pick

outliers must be removed or adjusted. Unstable location solutions based on events with few picks are also assessed to see if the addition of marginal phases will improve the stability of the location determination. After any required pick adjustments have been made, the events are then relocated, and combined with error information to allow ranking of the confidence of location quality.

These procedures have all been put in place and tested for the new HRSN configuration. Currently we have located 13 months of local earthquakes recorded by the new HRSN (over 2200 events) and are moving backwards in time to pick and locate the earlier data collected since March of 2001. We currently have enough data and are confident enough with the procedures to begin organizing the locations for formal inclusion into the NCEDC dbms and dissemination to the community. These efforts are now underway. We are also in the early stages of establishing a scalar seismic moment catalog for the new HRSN events that is also to be included in the NCEDC dbms.

Catalog Assessment. We continue to examine the earthquake data in search of possible earthquake precursors. This includes quality control and evaluation of the routine earthquake catalog locations and analyses of the spatial and temporal distribution of the microseismicity in relation to the occurrence of larger earthquakes in the area and heightened alert levels declared as part of the Parkfield Prediction Experiment. The new data and event detection scheme allows complete event detection down to ~ magnitude 0.0. As a result, the rate of earthquake detection by the HRSN exceeds that of the NCSN by about a factor of 5 in the 30 km stretch of the SAF centered at the location of the 1966 M6 Parkfield event. The additional rate of HRSN event detection significantly increases both the spatial and temporal resolution of the changing seismicity patterns and provide unique additional information on the earthquake pathology at very low magnitudes.

Post-San Simeon Processing.

Because of its mandate to detect and record very low magnitude events in the Parkfield area, the HRSN is extremely sensitive to changes in very low amplitude seismic signals. As a consequence, in addition to detecting very small local earthquakes at Parkfield, the HRSN also detects numerous regional events. Since the beginning of the network's data collection in 1987, the local and regional events were discriminated based on analyst assessment of S-P times, and only local events with S-P times less than ~ 2.5 sec at the first arriving station were picked and located as part of the HRSN routine catalog. Following the occurrence of the M6.5 San Simeon earthquake on December 22, of 2003, the long-standing data handling procedure outlined in the previous section was no longer viable due to the enormous rate of San Simeon aftershock detections (Figures 4 and 5). In the first 5 months following the mainshock, over 70,000 event detections were made by the HRSN system (compared to a yearly average detection rate of 6000 prior to San Simeon), and spot checks of the continuous 20 sps data revealed that the overwhelming majority of these detections resulted from seismic signals generated by San Simeon's aftershocks.

Data from the California Integrated Seismic Network (CISN) show that there were ~ 1,150 San Simeon aftershocks with magnitudes $>$ 1.8 occurring in the week following the mainshock. During this same period, the number of event detections from the HRSN was ~ 10,500 (compared to an average weekly for the year prior to San Simeon of 115 detections/per week). This suggests that the HRSN is detecting San Simeon aftershocks well below magnitude

1, despite the network's ~ 50 km distance from the mainshock (Figures 4 and 5).

The dramatic increase in event detections vastly exceeded the HRSN's capacity to process both the continuous and triggered event waveform data. To prevent the loss of seismic waveform coverage, processing of the triggered waveform data has been suspended to allow archiving of the 250 sps continuous data to tape to continue uninterrupted. Cataloging of the event detection times from the modified REDI real-time system algorithm is also continuing, and the 250 sps waveform data is currently being periodically uploaded from the DLT tapes onto the NCEDC for access to the research research community. Research funding has also been requested from NSF-EarthScope to develop and apply new techniques to process these continuous data with the aim of identifying the Parkfield local events from among the San Simeon aftershocks and of compiling waveform and location catalogs for the local earthquakes.

Recent Findings

Deep Fault Slip. Understanding the regional time-varying deformation field of fault zones at seismogenic depths is important for understanding active tectonics, fault interactions and the occurrence of large earthquakes (Stein, 1999; Freed and Lin, 2001; Bowman et al., 1998). However, measurements of time-varying deep deformation on a large-scale have been difficult to obtain due to the limited coverage of geodetic networks and the fundamental trade-offs and assumptions required to infer deep slip rates from measurements of surface motion (Langbein et al., 1999; Burgmann et al., 2000; Murray et al., 2000). Previously our research team pioneered a technique for using recurrence interval variations from characteristic microearthquake event sequences (over 40 % of the entire microearthquake population at Parkfield) to map fault slip rate variations at depth on fault surfaces (Nadeau and McEvilly, 1999). This technique has now gained broad acceptance in the seismologic community and it appears to be generally applicable to faults in a variety of tectonic environments (Burgmann et al., 2000; Templeton et al., 2001; Igarashi et al., 2003; Uchida et al., 2003; Chen et al., 2003). Several of these studies have also used repeating earthquakes to increase the scale, continuity, and resolution of deep aseismic slip information in regions where geodetic coverage is limited and where the depth resolution of geodetic inversions are low.

Along a 175 km segment of the central San Andreas Fault (SAF) (Figure 6), aseismic slip had long been thought to occur at a relatively constant rate modulated by localized slip transients induced by large earthquakes (USGS Prof. Pap. 1515, 1990; Scholz, 1990). However, large-scale geodetic measurements along this segment of fault have primarily been made in campaign surveys having long sampling intervals and, consequently, limited temporal resolution. Measurements with shorter interval sampling and greater temporal resolution have also been made within this region but only in limited areas (i.e., primarily around San Juan Bautista and Parkfield, CA). A number of recent studies using such measurements from Parkfield and San Juan Bautista have found large aseismic transients that are not directly associated with large earthquakes (Gwyther et al., 1996; Linde et al., 1996; Langbein et al., 1999; Nadeau and McEvilly, 1999; Gao et al., 2000; Gwyther et al., 2000; Bokelmann and Kovach, 2003).

In an effort to more clearly understand the role of these local transients in the context of the larger scale deep deformation occurring along the central SAF, Nadeau and McEvilly (2004) (N&M) used the repeating earthquake technique to infer deep fault slip along the 175 km segment using data from microearthquakes recorded by the surface regional Northern California

Seismic Network (NCSN) and borehole High Resolution Seismic Network at Parkfield (HRSN) between 1984 and 1999 (inclusive). The technique first identifies sequences of characteristically repeating small earthquakes (CS) and then uses their recurrence time and magnitude information to infer aseismic fault slip rates at seismogenic depths (Nadeau and McEvilly, 1999).

The N&M study revealed that the San Juan Bautista and Parkfield transients were actually part of a larger scale pattern of transient behavior and that over much of the region aseismic transients (pulses) recurred quasi-periodically (Figure 7). In the northwestern ~80 km portion of N&M's study segment, the quasi-periodic pulsing had a recurrence period of ~ 3 years and was generally coherently timed along the entire ~ 80 km portion. Moderate earthquakes (M>3.5) were rare in the southeastern ~30 km of this 80 km zone, but along the northwestern 50 km portion, 67 moderate sized events occurred during the study period. N&M found that the occurrence rate of these earthquakes was 6 to 7 times greater during the 1-year onset periods of the 3-year pulses compared to their occur rate over the remaining 2 years of the pulse cycles. They also found that the onset of the pulse in late 1989 corresponded to the occurrence of the M7.1 Loma Prieta earthquake that occurred just to the northwest of the study zone. The occurrence of the series of 3 slow earthquakes in the San Juan Bautista area (Linde et al., 1996; Gwyther et al., 2000) also correlated with the onsets of the 3-year pulses.

Immediately southeast of this 80 km section and extending for ~ 50 km, Nadeau and McEvilly also observed quasi-periodic pulsing (Figure 7). The timing of the pulses within this central section of the study zone were also generally coherently timed but had a shorter, 1.7 yr., recurrence period and the pulsing pattern in this zone did not correlate with the pattern observed to the northwest. In the southeastern-most 45 km of the study segment (including the greater Parkfield area), the transient pattern of aseismic slip changed again. Transients in this section are large, but show little evidence of periodicity (with the possible exception of the extreme southeast portion). N&M noted that though pulse timing was generally coherent in the northwestern 80 km zone, significant modulations among the pulses' amplitudes existed and that short-term disruptions in pulse timing occurred locally in some areas. They pointed out that these anomalies correlated in space with significant structural features in the seismogenic crust (i.e., the 1989 Loma Prieta earthquake rupture zone immediately to the northwest, the 1998 San Juan Bautista rupture zone and the juncture region of the Calaveras and SAF zones), and they suggested that the anomalies may have resulted from processes associated with these features.

In order to explain the fact that the timing of the pulsing remained coherent along the fault zone on either side of the local timing disruptions and in spite of strong local amplitude modulations, they speculated that a large scale quasi-periodic deformation process was taking place deep beneath the seismogenic zone in this area and was driving the quasi-periodic component of seismogenic zone deformation revealed by the repeating earthquake data. In this model, local anomalies in the repeating quake slip rates were explained by localized regions of strain accumulation and episodic release in the seismogenic zone (e.g., earthquake locked zones) or by the sharing/interaction of deformation on proximal faults responding to larger-scale deep deformation (e.g., at the Calaveras SAF juncture). N&M suggested that this deep pulsing source model could also explain the distinctly different pulsing pattern seen in the central 50 km of the study zone if a different pulsing source region existed deep under this segment and operated independently of the deep source region in the northwest. They also suggested that a deep pulsing source region might underlie the Parkfield section of the study zone, and that if this were the case shielding effects associated with the M6 locked zone might be substantially modifying

the deep slip signal to produce the transient signal seen in the repeating earthquake data.

In part, N&M's justification for the deep driving source model comes from analogy with the deep slow-slip event phenomena observed in the Cascadia region (where deep quasi-periodic aseismic deformation was observed in the subduction zone beneath the Cascadia megathrust at ~ 25-45 km depth) (Dragert et al., 2001; Miller et al., 2002) and deep similar phenomena in the subduction zones off Japan (Ozawa et al., 2001 and 2002; Shibazaki and Yoshihisa, 2003).

Fault Zone Guided Wave Analysis. Numerical modeling studies and a growing number of observations have argued for the propagation of fault-zone guided waves (FZGWs) within a San Andreas Fault (SAF) zone that is 100-200m wide at seismogenic depths and with 20% to 40% lower shear-wave velocity than the adjacent unfaulted rock. Using thousands of microearthquakes recorded since 1987 by the HRSN to characterize FZGW propagation in the SAF zone, Korneev et al. (2003) have imaged the FZGW attenuation structure of the innermost fault zone. They confirmed that FZGWs at Parkfield are generated within the fault zone (FZ) and that they are most prominent late in the coda of S. Numerical waveform modeling ad guided-wave amplitude tomograpic inversion show clearly that FZGWs are significantly less attenuated in a well-defined region of the FZ (Figure 8). This region plunges to the northwest along the northwest boundary of the region of highest moment release and separates locked and slipping sections of the SAF at depth, as determined independently from geodesy, seismicity, and the recurrence rates of characteristically repeating microearthquakes. We interpret this localized zone of strong FZGW propagation to be the northwest edge of the M6 asperity at Parkfield. The mechanism for low FZGW attenuation in the zone is possibly due to dewatering by fracture closure and/or fault-normal compression or changes in fracture orientation due to a complex stress or strain field at the boundary between creeping and locked zones of the SAF.

Migration of Seismic Scatterers. A collaborative effort with researchers at the Department of Terrestrial Magnetism (Carnegie) using repeating microearthquake sources at Parkfield has revealed the existence of time-varying seismic scatterers, and that this phenomena can be attributed to the stress induced evolution of crustal fractures (Niu et al., 2003). Using seismograms of repeating quakes recorded by the HRSN from 1987 through 1997, we found temporal variations in the seismograms that analyses reveal can be attributed to scatterer location changes of the order of 10 m for scatterers located ~ 3 km below the surface. We found that the motion of the scatterers is coincident, in space and time, with the onset of the well-documented aseismic transient in the area, and speculate that this structural change is the result of a stress-induced redistribution of fluids in the fluid-filled fractures caused by the transient event.

SAFOD Characterization. Another principal focus of BSL's recent research at Parkfield has been the detailed analysis and monitoring of the characteristics of microseismicity with in the drilling and penetration zone of the SAFOD component of the NSF initiative EarthScope. Of particular interest is the evolution of fault zone deformation and detailed seismic structure immediately surrounding the repeating SAFOD M2 target zone, and the recurrence behavior and size of the two potential M2 targets (separated by 70m).

Using a 3-dimensional double-difference code developed by Alberto Michelini in Italy and a preexisting 3-D cubic splines interpolated velocity model developed from HRSN data (Michelini and McEvilly, 1991), large numbers of small earthquakes were used to characterize the detailed structure and kinematics of the fault and the recurrence interval scaling properties of repeating micro-seismicity in a 4 x 4 km lateral and 6 km deep crustal volume surrounding the SAFOD

experiment's deep drilling zone (Nadeau et al., 2004) (Figure 9, top-left and top-right). The relocations indicate that the sub horizontally drilled portion of the SAFOD hole may need to penetrate a seismically active (and the existence of CS imply actively slipping) strand some 300 m to the SW before entering the M2 target region. Fifty-two CS exist on the SAF in the study area and have been used to infer deep slip rates on the fault using their recurrence properties (Nadeau and McEvilly, 1999). CS on the two actively slipping strands indicate that both strands are slipping at about 10 to 15 mm/yr. This suggests a distinct possibility of shearing of the deep borehole casing on the SW strand which needs to be taken into account if long term monitoring of the local target area is to take place.

The recurrence properties of the two repeating target event sequences were also characterized using both HRSN and Northern California Seismic Network (NCSN) data (Figure 9, bottom)). Since 1984 both of the ~ M2 sequences have had 7 events occur. The average magnitude of events in the northwestern-most sequence is M2.1 and the sequence has a mean recurrence interval of ~ 2.89 years with a coefficient of variation of 0.11. The last event in the sequence occurred on ~ 2003.80 (i.e., Oct. 20, 2003) and based on the recurrence statistics the next events is expected on ~ 2006.69 (+/- 0.32 years, 1 standard deviation). The average magnitude of the southeastern-most sequence is M1.9 and its recurrence intervals also have a mean of ~2.89 years but with a coefficient of variation of 0.17. The last event in this sequence occurred on 2003.80 (i.e., Oct. 21, 2003), and based on the recurrence statistics the sequence's next event is also expected on ~ 2006.69 (+/- 0.49 years, 1 standard deviation).

The recurrence properties of both ~M2 sequences are consistent with the recurrence scaling of the other sequences in the study zone. This scaling, however, is contrary to that expected from standard constant stress-drop theory (Figure 10). SAFOD's 'in-situ' measurements of fault zone processes and its near-field seismic observations of repeating M2 earthquake sequences should soon provide the information needed to resolve the apparent discrepancy between the observed and expected microearthquake recurrence behavior.

Earthquake Distributions: Fractals, b-values and Asperities. In collaboration with researchers at the World Agency of Planetary Monitoring and Earthquake Risk Reduction, the University of Southern California and the Institute of Geophysics (ETH Hoenggerberg) in Switzerland, we have used seismicity data in the Parkfield area to test the hypotheses (1) that the fractal dimension, D, of hypocenters are different in a locked and a creeping segment of the San Andreas fault and (2) that the relationship $D \sim= 2b$ holds approximately, where b is the slope of the frequency-magnitude relationship (Wyss et al., 2004). We found that in the locked portion of the SAF at Parkfield $0.5 < b < 0.7$ and $0.96 < D < 1.14$, whereas in the creeping segment, $1.1 < b < 1.6$ and $1.45 < D < 1.72$. However, the spatial distribution of the hypocenters in the creeping segment is not well approximated by a fractal distribution. We conclude (1) that the frequency-magnitude distribution as described by b, as well as the fractal dimension (D), are different in the locked and creeping segments near Parkfield; (2) that the spatial distribution in the creeping segment is not well approximated by a fractal distribution; and (3) that the relationship $D \sim= 2b$ holds in the locked segment, where both parameters can be measured accurately. Thus, we propose that the heterogeneity of seismogenic volumes lead to differences in D and b and that these differences, where established by high-quality data, may furnish clues concerning properties of fault zones.

Acknowledgments

Thomas V. McEvilly, who passed away in February 2002, was the PI on the HRSN project for many years. Without his dedication the creation and of the HRSN would not have been possible. Under Bob Nadeau's general supervision, Rich Clymer, Douglas Dreger, Bob Uhrhammer, Doug Neuhauser, Don Lippert, Bill Karavas, John Friday, and Pete Lombard all contribute to the operation of the HRSN. The NSF provided support during the 2000-2003 period for the SAFOD expansion of the HRSN through grant EAR-9814605.

References

Bakun, W.H., and A.G. Lindh, The Parkfield, California, prediction experiment, *Earthq. Predict. Res.,* 3, 285-304, 1985.

Beeler, N.M., D.L. Lockner, and S.H. Hickman, A simple stick-slip and creep-slip model for repeating earthquakes and its implications for microearthquakes at Parkfield, *Bull. Seism. Soc. Am.*, 91, 1797-1804, 2001.

Bokelmann, G.H.R. and R.L. Kovach, Long-term creep-rate changes and their causes, Geophys. Res. Lett., 30(8), 1445, doi:10.1029/2003GL017012, 2003.

Bowman, D.D., Ouillon, G., Sammis, C.G., Sornette, A., and Sornette, D., An observational test of the critical earthquake concept, *J. Geophys. Res.,* 103, 24359-24372, 1998.

Bürgmann, R., D. Schmidt, R.M. Nadeau, M. d'Alessio, E. Fielding, D. Manaker, T.V. McEvilly, and M.H. Murray, Earthquake Potential along the Northern Hayward Fault, California, *SCIENCE*, 289, 1178-1182, 2000.

Chen, H., and R. Rau, Fault slip rates from repeating microearthquakes on the Chihshang fault, eastern Taiwan, EOS Trans. AGU, 84(46), Fall Meet. Suppl., Abstract T11F-06, 2003.

Dragert, H., W. Kelin, and T.S. James, A silent slip event on the deeper Cascadia subduction interface, Science, 292, 1525-1528, 2001.

Freed, A.M., and J. Lin, Delayed triggering of the 1999 Hector Mine earthquake by viscoelastic stress transfer, Nature, 411, 180-183, 2001.

Gao, S.S., P.G. Silver, and A.T. Linde, Analysis of deformation data at Parkfield, California: detection of a long-term strain transient, J. Geophys. Res., 105, 2955-2967, 2000.

Gwyther, R.L., M.T. Gladwin, M. Mee and R.H.G. Hart, Anomalous shear strain at Parkfield during 1993-94, Geophys. Res. Lett., 23, 2425-2428, 1996.

Gwyther, R.L., C.H. Thurber, M.T. Gladwin, and M. Mee, Seismic and Aseismic Observations of the 12th August 1998 San Juan Bautista, California, M5.3 Earthquake, in Proceedings of the 3rd Conference on tectonic problems of the San Andreas Fault system, G. Bokelmann and R. Kovach, Eds., Stanford California School of Earth Sciences, Stanford University, 2000.

Harris, R., and P. Segall, Detection of a locked zone at depth on the Parkfield, California segment of the San Andreas fault, *J. Geophys. Res.*, *92*, 7945-7962, 1987.

Igarashi, T., T. Matsuzawa, and A. Hasegawa, Repeating earthquakes and interplate aseismic slip in the northeastern Japan subduction zone, J. Geophys. Res., 108, 2249, doi:10.1029/2002JB001920, 2003.

Johnson, L.R. and R.M. Nadeau, Asperity Model of an Earthquake: Static Problem, *Bull. Seism. Soc. Am.,* 92, 672-686, 2002.

Karageorgi, E., R. Clymer and T.V. McEvilly, Seismological Studies at Parkfield: II. Search for temporal variations in wave propagation using Vibroseis, *Bull. Seism. Soc. Am.,* 82, 1388-1415, 1992.

Karageorgi, E.D., T.V. McEvilly and R.W. Clymer, Seismological Studies at Parkfield IV: Variations in Controlled-Source Waveform Parameters and Their Correlation With Seismic Activity, 1987-1994, Bull. Seism. Soc. Am., **87**, 39-49, 1997.

Korneev, V.A., T.V. McEvilly and E.D. Karageorgi, Seismological Studies at Parkfield VIII: Modeling the Observed Controlled-Source Waveform Changes, Bull. Seism. Soc. Am. **90**, 702-708, 2000.

Korneev, V.A., R.M. Nadeau and T.V. McEvilly, Seismological Studies at Parkfield IX: Fault-Zone Imaging Using Guided Wave Attenuation, Bull. Seism. Soc. Am. 93, 1415-1426, 2003.

Langbein, J., R.L. Gwyther, R.H.G. Hart, and M.T. Gladwin, Slip-rate increase at Parkfield in 1993 detected by high-precision EDM and borehole tensor strainmeters, Geophys. Res. Lett., 26, 2529-2532, 1999.

Linde, A. T., M. T. Gladwin, M. J. S. Johnston, et al., A slow earthquake sequence on the San Andreas fault, Nature 383, 65-68, 1996.

Michelini, A. and T.V. McEvilly, Seismological studies at Parkfield: I. Simultaneous inversion for velocity structure and hypocenters using B-splines parameterization, *Bull. Seism. Soc. Am.,* 81, 524-552, 1991.

Miller, M.M., T. Melbourne, D.J. Johnson, and W.Q. Sumner, Periodic slow earthquakes from the Cascadia subduction zone, *Science*, *295*, 2423, 2002.

Murray, J., P. Segall, P. Cervelli, W. Prescott, and J. Svarc, Inversion of GPS data for spatially variable slip-rate on the San Andreas fault at Parkfield, CA, Geophys. Res. Lett., 28, 359-362, 2001.

Nadeau, R. M. and L. R. Johnson, Seismological Studies at Parkfield VI: Moment Release Rates and Estimates of Source Parameters for Small Repeating Earthquakes, *Bull. Seism. Soc. Am., 88,* 790-814, 1998.

Nadeau, R. M. and T. V. McEvilly, Fault slip rates at depth from recurrence intervals of repeating microearthquakes, *Science* 285, 718-721, 1999.

Nadeau, R.M. and T.V. McEvilly, Periodic Pulsing of Characteristic Microearthquakes on the San Andreas Fault, *Science,* 303, 220-222, 2004.

Nadeau, R.M., A. Michelini, R.A. Uhrhammer, D. Dolenc, and T.V. McEvilly, Detailed kinematics, structure and recurrence of micro-seismicity in the SAFOD target region, Geophys. Res. Lett., 31, (in press), doi:10.1029/2003GL019409, 2004.

Niu, F., P.G. Silver, R.M. Nadeau and T.V. McEvilly, Migration of seismic scatterers associated with the 1993 Parkfield aseismic transient event, Nature, 426, 544-548, 2003.

Oye, V., J.A. Chavarria and P.E. Malin, Determining SAFOD area microearthquake locations solely with Pilot Hole seismic array data, Geophys. Res. Lett., 31, L12S10, doi:10.1029/2003GL019403, 2004.

Ozawa, S., M. Murakami, and T. Tada, Time-dependent inversion study of the slow thrust event in the Nankai trough subduction zone, southwestern Japan, J. Geophys. Res., 106, 787-802, 2001.

Ozawa, S., M. Murakami, M. Kaidzu, T. Tada, T. Sagiya, Y. Hatanaka, H. Yarai, T. Nishimura, Detection and Monitoring of Ongoing Aseismic Slip in the Tokai Region, Central Japan, Science, 298, 1009-1012, 2002.

Roecker, S., C. Thurber and D. McPhee, Joint inversion of gravity and arrival time data from Parkfield: New constraints on structure and hypocenter locations near the SAFOD drillsite, Geophys. Res. Lett., 31, L12S04, doi:10.1029/2003GL019396, 2004.

Scholz, C.H., The mechanics of earthquakes and faulting, 439 pp., Cambridge University Press, Cambridge, 1990.

Shibazaki, B. and I. Yoshihisa, On the physical mechanism of silent slip events along the deeper part of the seismogenic zone, Geophys. Res. Lett., 30(9), 1489, doi:10.1029/2003GL017047, 2003.

Stein, R.S., The role of stress transfer in earthquake occurrence, Nature, 402, 605-609, 1999.

Templeton, D.C., R.M. Nadeau and R. Bürgmann, Structure and kinematics at the juncture between the San Andreas and southern Calaveras faults, Eos Trans. AGU, 82, F881, 2001

Thurber, C., S. Roecker, H. Zhang, S. Baher and W. Ellsworth, Fine-scale structure of the San Anbdreas fault zone and location of the SAFOD target earthquakes, Geophys. Res. Lett., 31, L12S02, doi:10.1029/2003GL019398, 2004.

Uchida, N., T. Matsuzawa, A. Hasegawa, and T. Igarashi, Interplate quasi-static slip off Sanriku, NE Japan, estimated from repeating earthquakes, Geophys. Res. Lett., 30, 1801, doi:10.1029/2003/GL017452, 2003.

Wallace, R.E. (ed.), The San Andreas Fault System, California, U. S. Geol. Surv. Prof. Pap., 1515, 283 pp., 1990.

Wenk, H.-R., L.R. Johnson, and L. Ratschbacher, Pseudotachylites in the Eastern Peninsular Ranges of California, *Tectonophysics,* 321, 253-277, 2000.

Wyss, M., C. G. Sammis, C.G., R.M. Nadeau and S. Weimer, Fractal Dimension and b-value on Creeping and Locked Patches of the San Andreas Fault near Parkfield, CA, Bull. Seism. Soc. Am., 94, 410-421, 2004.

Bibliography

Korneev, V.A., R.M. Nadeau and T.V. McEvilly, Seismological Studies at Parkfield IX: Fault zone Imaging using Guided Wave Attenuation, *Bull. Seismol. Soc. Am.,* 93, 1415-1426, 2003.

Nadeau, R. M. and T. V. McEvilly, Periodic Pulsing of Characteristic Microearthquakes on the San Andreas Fault, *Science,* 303, 220-222, 2004.

Nadeau, R.M., A. Michelini, R.A. Uhrhammer, D. Dolenc, and T.V. McEvilly, Detailed kinematics, structure, and recurrence of micro-seismicity in the SAFOD target region, *Geophys. Res. Lett.,* 31, L12S08, doi:10.1029/2003GL019409, 2004.

Niu, F., P.G. Silver, R.M. Nadeau and T.V. McEvilly, Migration of seismic scatterers associated with the 1993 Parkfield aseismic transient event, *Nature,* 426, 544-548, 2003.

Wyss, M., C. G. Sammis, C.G., R.M. Nadeau and S. Weimer, Fractal Dimension and b-value on Creeping and Locked Patches of the San Andreas Fault near Parkfield, CA, *Bull. Seism. Soc. Am.,* 94, 410-421, 2004.

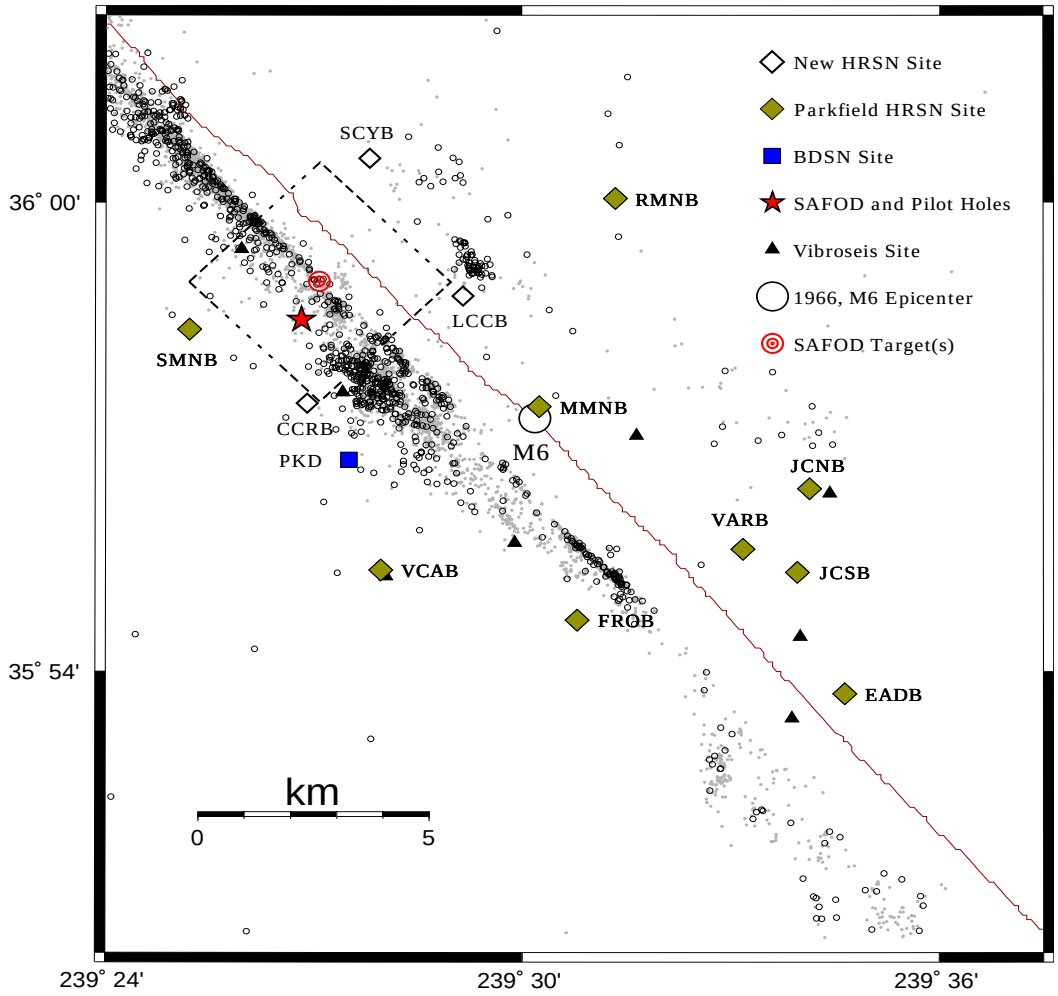

Figure 1. Map showing the San Andreas Fault trace, the location of the original 10 Parkfield HRSN stations (filled diamonds) and the 3 new sites (open diamonds) installed to enhance coverage around the SAFOD facility. Station GHIB (Gold Hill, not shown) is located on the San Andreas Fault about 8 km to the Southeast of station EADB. The location of the BDSN broadband station PKD is also shown (filled square). The location of the SAFOD pilot hole and main drill site are shown by the filled star. Location of the 2 alternative M2 repeating earthquake targets (70 meters apart) are shown as concentric circles. Because of the SAFOD experiment, the 4 km by 4 km dashed box surrounding the SAFOD zone is a region of particular interest to BSL researchers. The epicenter of the 1966 M6 Parkfield main shock is located at the large open circle. Routine locations of earthquakes recorded by the expanded and upgraded 13 station HRSN are shown as open black circles. Locations of events recorded by the earlier vintage 10 station HRSN, relocated using an advanced 3-D double-differencing algorithm applied to a cubic splines interpolated 3-D velocity model (Michelini and McEvilly, 1991), are shown as gray points. The locations of the 8 source points for the Vibroseis wave propagation monitoring experiment (Karageorgi et al., 1992, 1997) are represented by small black triangles.

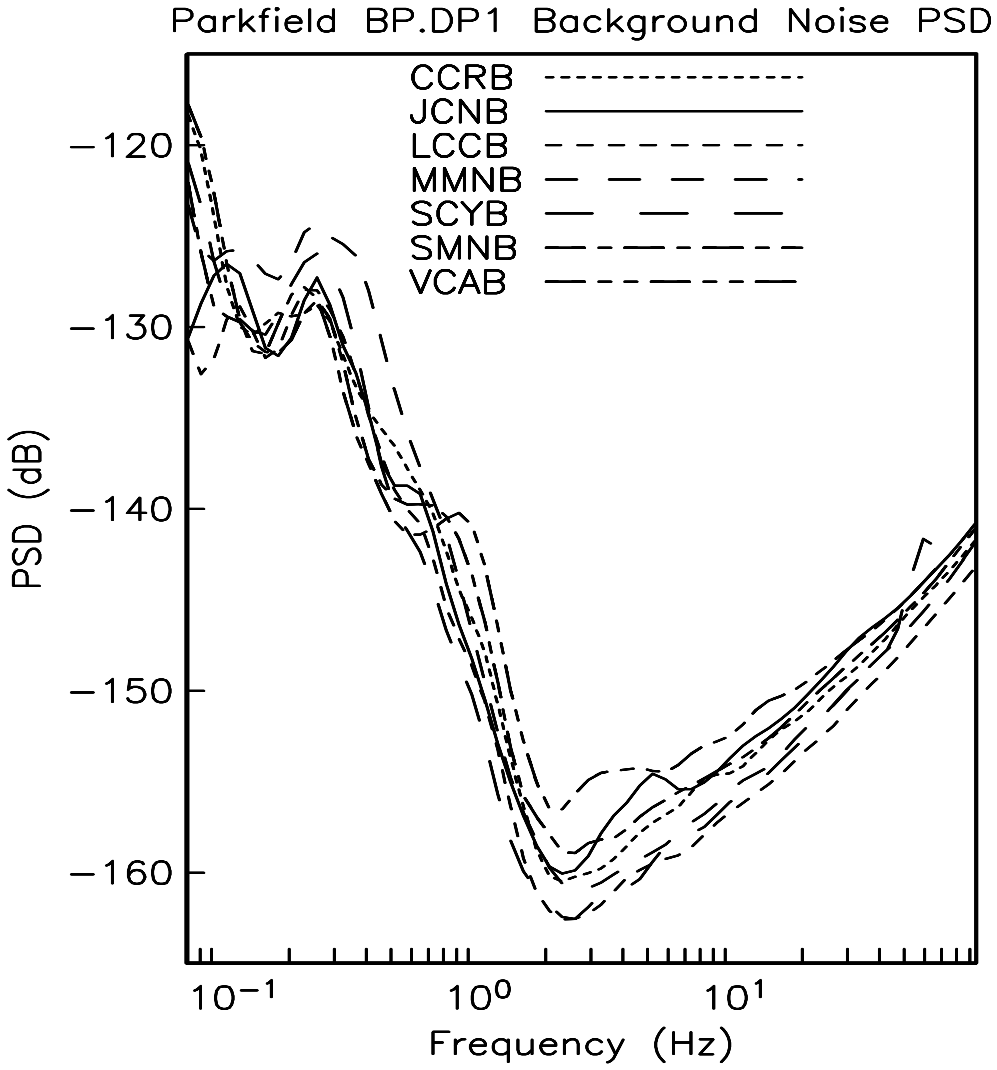

Figure 2. Background noise PSD plot for the seven continuously telemetered BP.DP1 data streams from Parkfield. The data are 20-minute samples starting at 2003.225.0900 (2 AM PDT). The plots show the background noise PSD as a function of frequency for the highest available sampling rate (250 sps) vertical component data which are continuously telemetered to Berkeley. Note the relatively low PSD levels and the overall consistency for all the HRSN stations. By comparison, PSD curves (not shown) among the borehole Northern Hayward Fault Network (NHFN) land and bridge stations are much more variable and show a generally higher background noise level. The differences between the PSDs for these two different networks can for the most part be explained by the relative cultural noise levels in the two areas, by the depth of the borehole sensors, and by whether the boreholes remain open holes (noisier) or have been filled with cement. The 2 Hz minimum in the PSD plots for the HRSN sensor results from the response of the 2 Hz sensors used for the HRSN. Below 2 Hz, noise levels rise rapidly and they peak at 3 sec (.3 Hz), which is characteristic of teleseismic noise observed throughout California. In the 2 to 5 Hz range, VCAB and JCNB have historically shown higher background noise, which is believed to result from excitation modes in the local structure and their vicinity to local road traffic. A small 60 Hz blip can be seen in the SCYB curve due to its close proximity to a power-line.

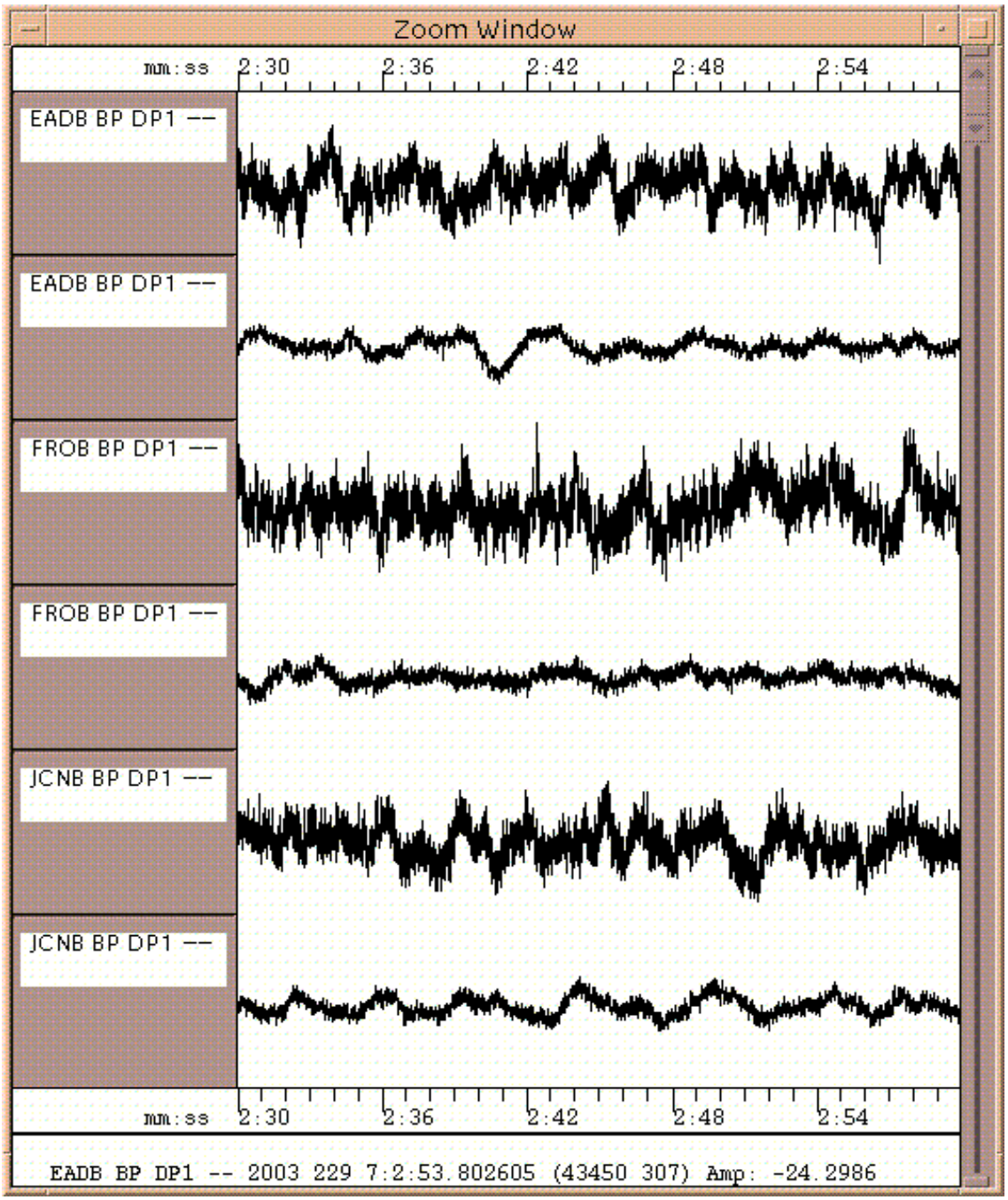

Figure 3. Preamp noise reduction test. Shown are 30 seconds of vertical background signal recorded at stations EADB, FROB and JCNB on day 229 of 2003 at 0700 UTC (top of station pairs, recorded at x80 gain and scaled up by 1000/80 for comparison to the x1000 preamp gain levels) and 0700 UTC on day 233 (bottom of station pairs, recorded at x1000 preamp gain). Note the substantial reduction in background noise, due primarily to the lower preamp generated noise at higher preamp gain.

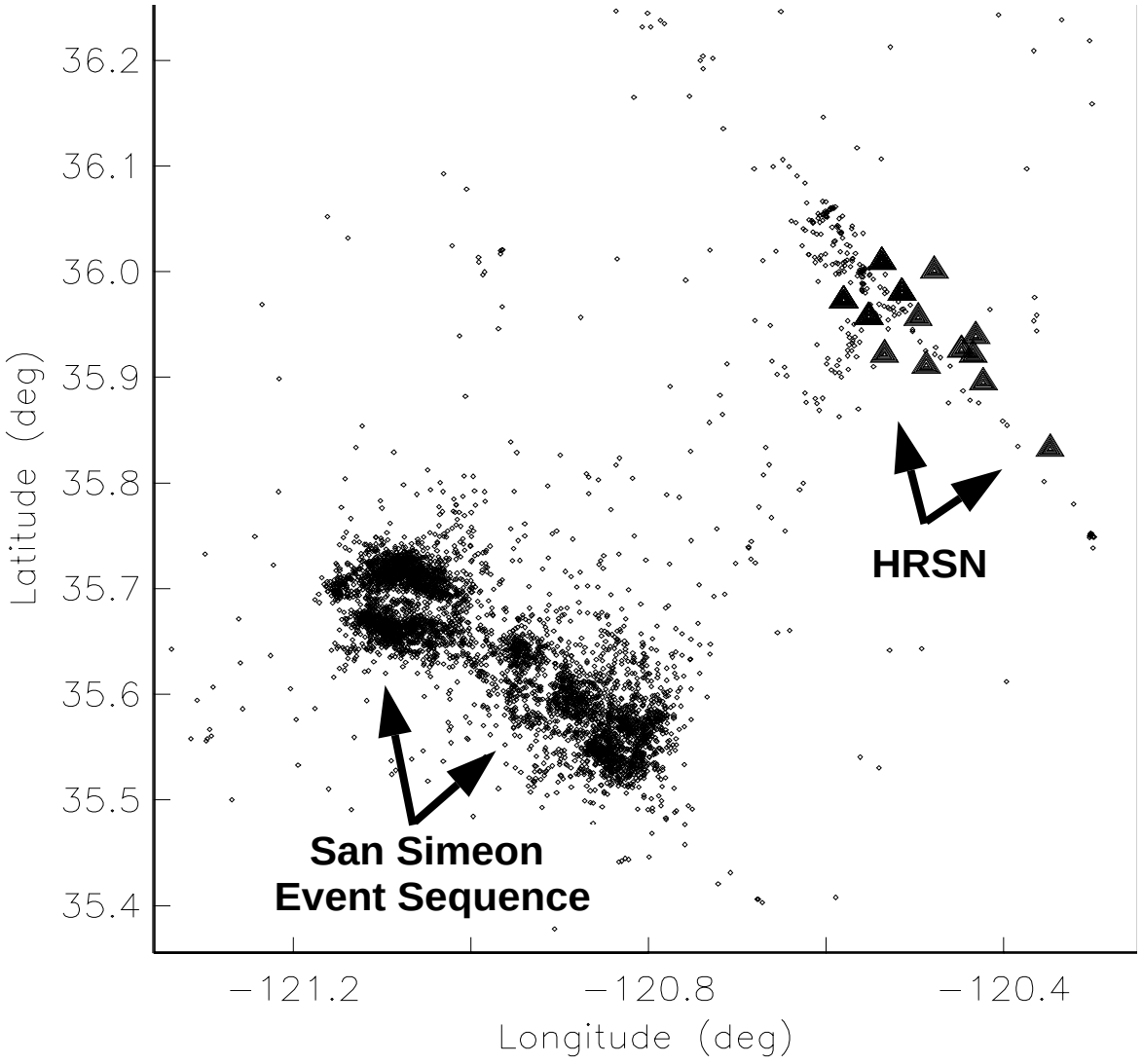

Figure 4. Earthquake locations of 5847 events in the San Simeon and Parkfield areas of California occurring between December 1, 2003 and April 1, 2004, inclusive (small black circles). Locations are from the Northern California Seismic Network catalog, which is complete down to M1.8 in the overall region. Black triangles are the stations of the borehole High Resolution Seismic Network (HRSN). The M6.5 San Simeon event of December 22, 2003 and its aftershocks occurred in a region approximately 40 to 50 km southwest of the HRSN. Prior to the mainshock, seismicity in this region was predominantly quiescent.

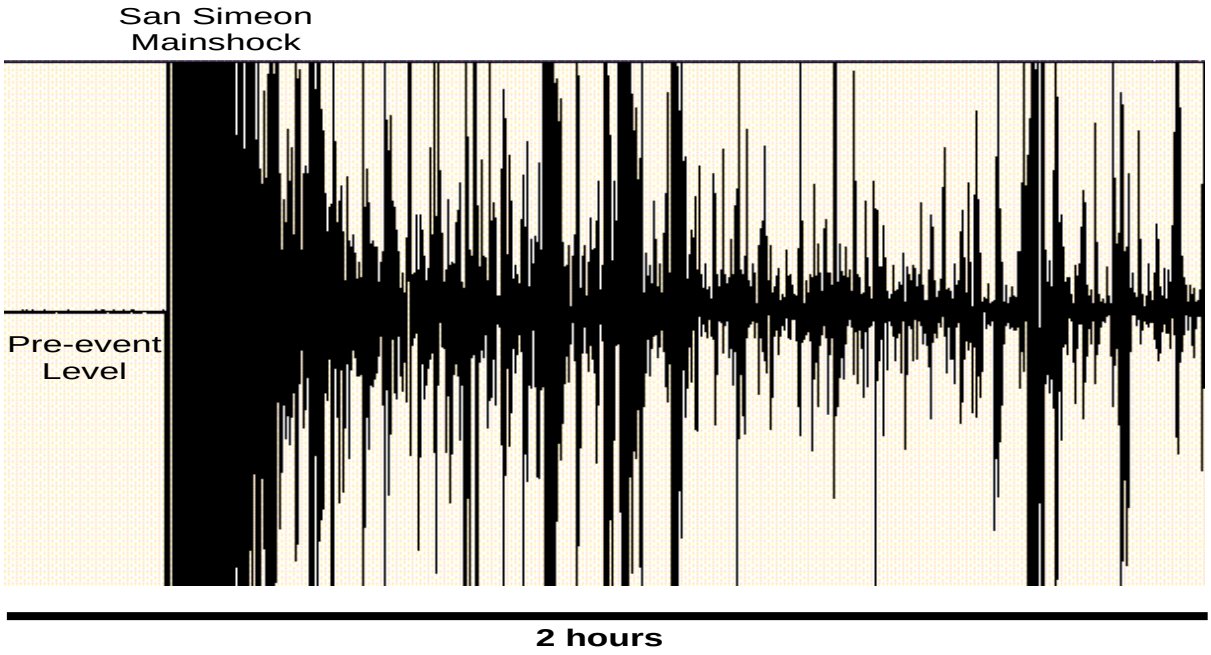

Figure 5. Unfiltered seismogram of the San Simeon mainshock and immediate aftershocks. Shown is a two-hour snapshot of continuous 250 sps data recorded by the vertical component of the borehole HRSN station SMNB (located ~ 50 km to the northeast of the mainshock). Approximately 15 minutes of background pre-event recording is shown before the mainshock. Following the mainshock seismic signal levels are elevated well above the background level almost continuously and signals from multiple aftershocks (and possibly Parkfield local events) generally overlap. The very low background noise recordings of the borehole HRSN stations and the networks high detection sensitivity (designed for detecting very low magnitude Parkfield local events) causes the network to trigger on 10's of thousands of distant and small San Simeon aftershocks (many below magnitude 1), this despite the HRSN's distance of ~ 50 km from the sequence.

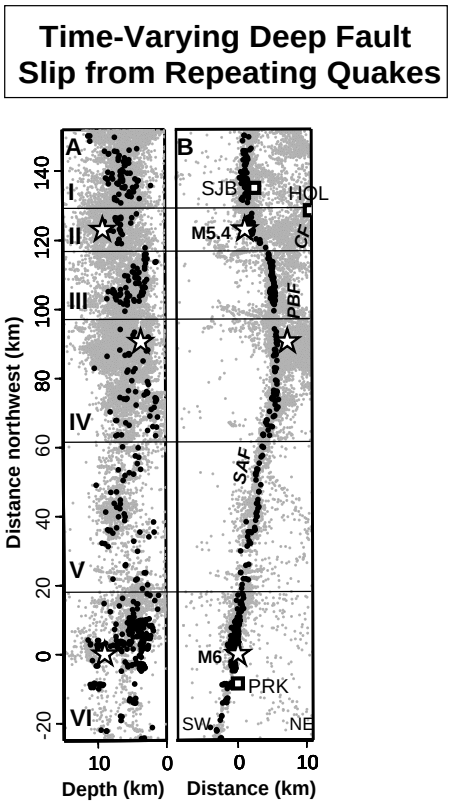

Figure 6. Locations of seismicity and characteristic sequences along the N&M study zone in depth section (**A**) and map view (**B**). Local coordinate system origin: lat 35.955 deg. N, long 120.495 deg. W, oriented N45:W. Depth and across fault scales exaggerated by 2. Black circles are locations of 515 CS (2594 events). Remaining seismicity are gray points. Horizontal lines delineate regions I - VI discussed in N&M. White stars are 1998 San Juan Bautista (M5.4), 1966 Parkfield (M6) and 1988 swarm of 500+ small earthquakes (on Paicines-San Benito fault (PBF)). White squares are cities of San Juan Bautista (SJB), Hollister (HOL) and Parkfield (PRK). Calaveras and San Andreas Fault seismicity are labeled CF and SAF, respectively.

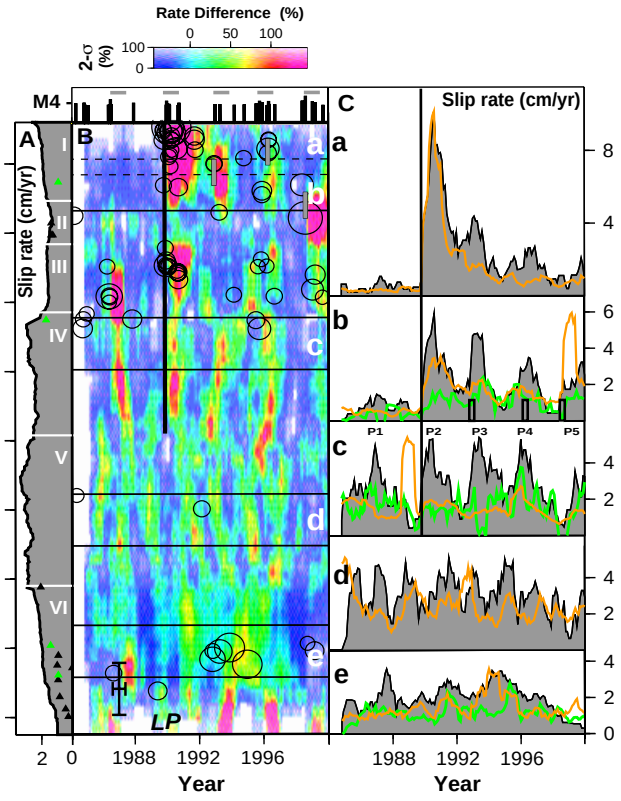

Figure 7. (**A**) Long-term slip rate profile of the central SAF. Triangles are locations and long-term rates from creepmeter data. Green triangles indicate creepmeters used for rate histories in (C). Regions I - VI correspond to Figure 6. (**B**) Profile of short-term rates in percent difference of long-term rates. Color intensities are 95% confidence bounds. Vertical black line is time of the M7.1 Loma Prieta earthquake. Open circles are times and relative sizes of earthquakes >M3.5. Three gray vertical bars in regions I and II are approx. locations, lengths and times of shallow silent slip events in the area (late 1992, early 1996 and mid-1998; Linde et al., 1996: Gwyther et al., 2000). Black barred cross in the lower left shows segment and time windows used for stacking. Lower case letters and horizontal black lines correspond to the five segments whose slip and seismicity rates are shown in (C) (dashed lines are overlapping regions of segments a and b). (Top) Time series of >M3.5 events (excluding Loma Prieta aftershocks) in regions I - III. Horizontal gray bars are 1 yr. pulse onset periods. (**C**) 0.8 year smoothed rate histories of repeating quake slip (gray), fault creep (green), and seismicity (orange) for segments a through e. Rectangles in segment b are times of silent slip events. P1 - P5 are pulse designations discussed in N&M. Seismicity rate pulses in segments b and c are from the M5.4 San Juan Bautista aftershock sequence and the 1988 event swarm on the PBF (Figure 6).

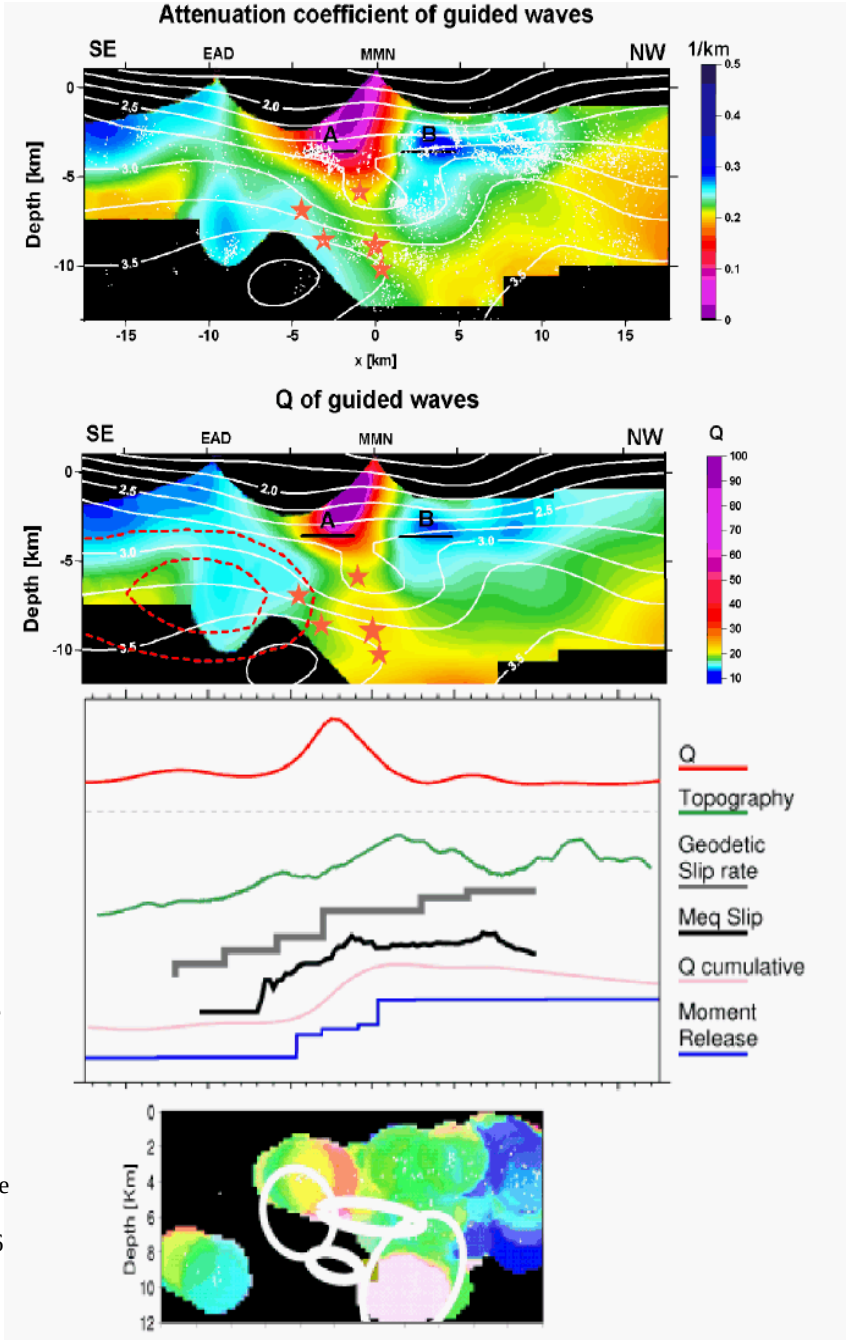

Figure 8. Spatial relationship of the FZGW attenuation/Q anomaly with other observations along the Parkfield segment of the San Andreas fault zone. Top 2 panels show in-fault attenuation and Q images resulting from the FZGW tomographic reconstructions. Not the NW-plunging zone of low FZGW attenuation (high Q) in the central portion of the panels delineating the transition at depth of locked to creeping fault. Also shown are Vs contours, 1987-1998 seismicity (white dots and small red stars for the 4 recent M>4 events), and the 1966 M6 hypocenter (large red star). The center panel shows the function of FZGW Q taken along a profile at 3 km depth. Shown immediately below the Q curve are curves representing topography along the fault (green), surface fault slip rates from geodetic data (Harris and Segall, 1987, in grey), slip rates in the depth range 0 to 5 km inferred from recurrence intervals of characteristic microearthquake sequences (black), the cumulative Q function taken along the fault segment (SE to NW, pink) and the 1987-1998 moment release as a cumulative function along the fault from SE to NW (blue). The bottom panel shows the along fault deep slip rate distribution at Parkfield inferred from the recurrence times of characteristic microearthquakes occurring between mid-1992 and 1995 (inclusive, see Nadeau and McEvilly, 1999), and the aftershock regions of the M>4 earthquakes occurring during this time period. Along fault features in all these characteristics correlate spatially and appear to delineate the transition from locked to creeping behavior on the surface and at depth on the SAF at Parkfield.

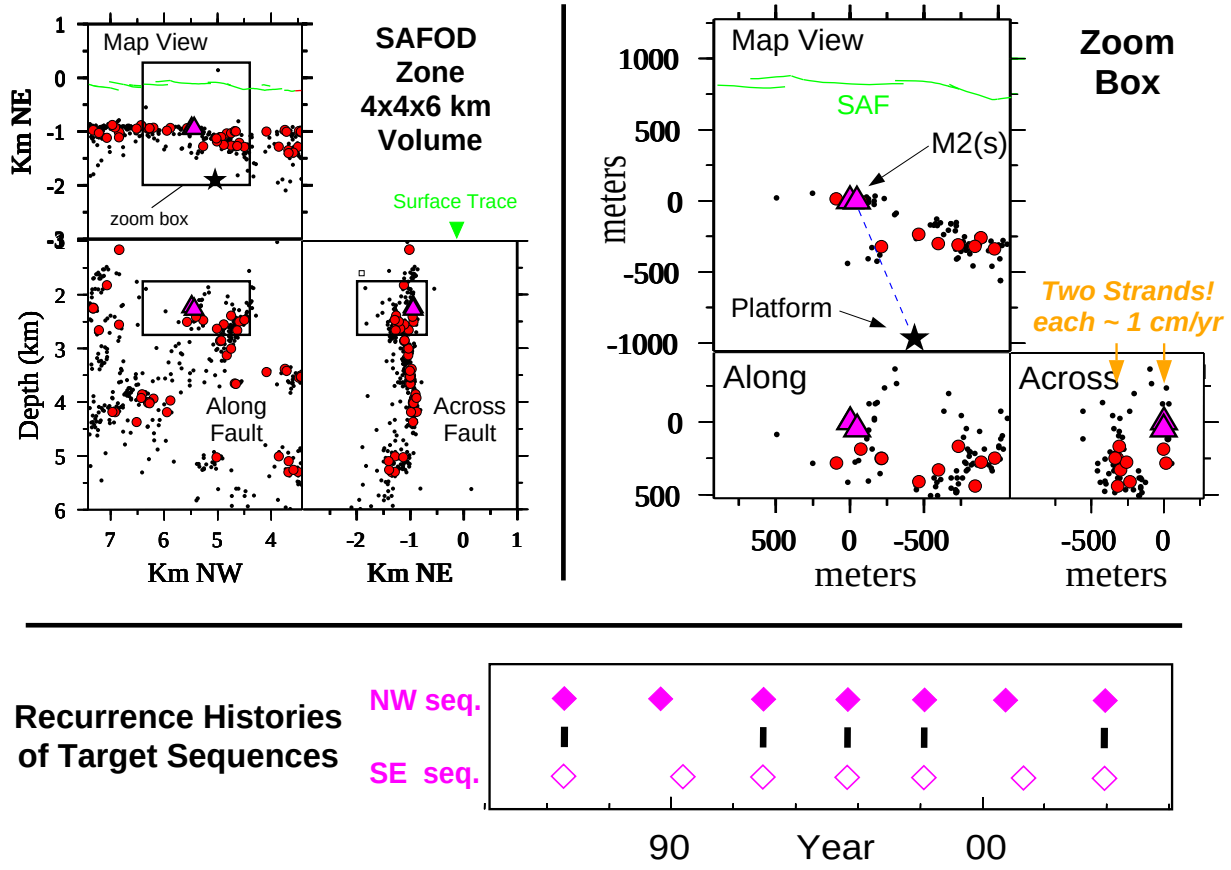

Figure 9. (UPPER LEFT PANEL) Relocated seismicity (black points) and sites of characteristically repeating microearthquake sequences (red circles) in the 4 by 4 by 6 km deep study volume containing the SAFOD M2 target(s) (purple triangles). (Top) Map view. (Bottom-left) Along fault depth section view with depths given relative to mean sea level (~ 600 m depth). (Bottom-right) Across fault depth section view. Trace of the San Andreas Fault is in green. Rectangles delineate the focus target zone in LEFT PANEL. Black star is the location of the SAFOD drilling platform.

(UPPER RIGHT PANEL) Double-difference relocated seismicity in the volume immediately surrounding the SAFOD target zone is shown in map view (top-left), along fault depth section view (bottom-left), and across fault depth section view (bottom-right). Purple triangles show the locations of the two SAFOD repeating event targets. Black points, red circles, purple triangles, and black star are as in the UPPER LEFT PANEL. Axis values are given in meters relative to the NW target sequence location. Orange arrows indicate the seismicity of the two fault strands separated by ~ 300 m discussed in the text as well as the other repeating sequences used in estimating the strands' deep fault creep rates.

(LOWER PANEL) Timelines of events in the two SAFOD target sequences NW (filled purple diamonds) and SE (open purple diamonds). Horizontal dashes indicate events in sequence NW that are followed within 24 hours by an event in sequence SE.

Recurrence Scaling and Fault Properties

(Competing Models)

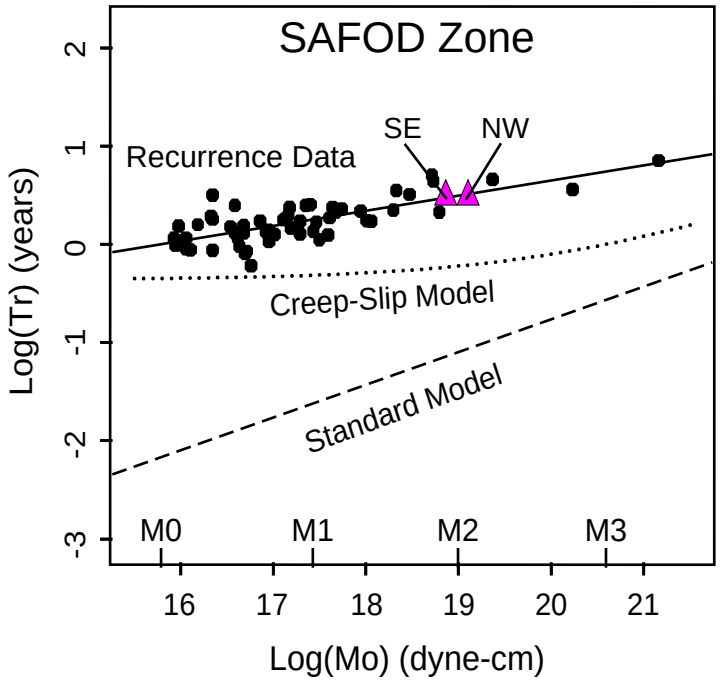

Figure 10. Scaling of the mean recurrence intervals (Tr) of the 52 characteristic sequences in the study area. Event sizes are given in NCSN preferred magnitude (M) and in seismic moment (for comparison with Nadeau and Johnson [1998]). Purple triangles are data points for the SAFOD repeating target sequences. Black circles are data from the remaining 50 repeating sequences in the area. Dotted line shows the creep-slip model from equation (14) of Beeler et al. [2001] for a 3 MPa constant stress-drop, a C parameter of 3.0 MPa/cm, and a loading velocity of 2.3 cm/yr. Using a 10 MPa stress-drop in this model shifts the creep-slip curve upward along the y-axis by ~0.52, putting the curve in general agreement with the sequence data. Dashed line shows the scaling expected from a 3 MPa standard constant stress-drop model assuming circular rupture. Black line shows the least squares fit to the characteristic sequence data. Its slope and intercept are 0.246 +/- 0.69 and 0.009 +/- 0.14 for magnitude or 0.154 +/- 0.43 and -2.424 +/- 0.14 in seismic moment.